Crystal Structure Theory and Applications, 2017, 6, 11-24
http://www.scirp.org/journal/csta
ISSN Online: 2169-2505
ISSN Print: 2169-2491

Synthesis, Structural Characterization and DFT Studies of Silver(I) Complex Salt of Bis(4,5-dihydro-1*H*-benzo[g]indazole)

Tanyi Rogers Fomuta[1], Golngar Djimassingar[1,2], Jean Ngoune[1*], Nana Odette Ngnabeuye[1], Jean Jacques Anguile[3], Justin Nenwa[4*]

[1]Department of Chemistry, University of Dschang, Dschang, Cameroon
[2]Department of Chemistry, Mongo Polytechnique University Institute (IUPM), Mongo, Chad
[3]Department of Chemistry, University of Sciences & Techniques of Masuku, Franceville, Gabon
[4]Department of Inorganic Chemistry, University of Yaounde 1, Yaounde, Cameroon
Email: *jean.ngoune@univ-dschang.org, *jnenwa@yahoo.fr

How to cite this paper: Fomuta, T.R., Djimassingar, G., Ngoune, J., Ngnabeuye, N.O., Anguile, J.J. and Nenwa, J. (2017) Synthesis, Structural Characterization and DFT Studies of Silver(I) Complex Salt of Bis(4,5-dihydro-1*H*-benzo[g]indazole). *Crystal Structure Theory and Applications*, **6**, 11-24.
https://doi.org/10.4236/csta.2017.62002

Received: May 10, 2017
Accepted: May 20, 2017
Published: May 28, 2017

Abstract

A new silver complex salt $[Ag(N_2C_{11}H_{10})_2]NO_3$ (where $N_2C_{11}H_{10}$ = 4,5-dihydro-1*H*-benzo[g]indazole), has been synthesized and characterized by elemental and thermal analyses, IR and ^{1}HNMR spectroscopies, single crystal X-ray structure determination and DFT studies. Its molecular structure comprises of a silver center coordinated to two nitrogen atoms from two 4,5-dihydro-1*H*-benzo[g]indazole molecule giving rise to a cationic complex entity, $[Ag(N_2C_{11}H_{10})_2]^+$ with NO_3^- as counter ion. The bulk structure is consolidated by N–H···O, C–H···π, Ag···π and Ag···O intermolecular interactions, thus generating a pseudo-helical network. The optimized structure, frontier molecular orbitals (HOMO and LUMO) and global reactivity descriptors were investigated by performing DFT calculations.

Keywords

Silver Complex Salt, 4,5-dihydro-1*H*-benzo[g]indazole, Hydrogen Bonds, Thermogravimetric Analysis, ^{1}HNMR, X-Ray, DFT Studies

1. Introduction

Pyrazole (Hpz) or 1,2-diazacyclopenta-2,4-diene is a heterocyclic five-membered ring compound containing three carbon atoms with two nitrogen atoms in adjacent positions. Over the past two decades, pyrazole-containing compounds have received considerable attention owing to the fact that pyrazoles exhibit antimicrobial [1] [2], anticancer [3], antibacterial [4] [5], antipyretic [6] and analgesic [7] activities. Moreover, they are suitable agents for investigating the active

sites of biomolecules and for modeling the biosystems of oxygen transfer [8]. The pyrazole moiety shows a broad game of chemical reactivity due to the presence of both the pyridine- and the pyrole-type nitrogen atoms, enabling it to act both as a Lewis acid and as a Lewis base. Electronic and steric effects can therefore be fine-tuned nearly at will by introducing various substituents on different carbon atoms on the ring or by substituting hydrogen atoms [9] [10] [11] to generate new pyrazole derivatives. Some of these pyrazoles are very promising for the synthesis of inorganic materials with particular properties such as luminescence and collective magnetic phenomena [12]-[15]. In particular, Trofimenko *et al.* [16] synthesized and characterized the pyrazole, 4,5-dihydro-1*H*-benzo[g]indazole, whose coordination chemistry is still less developed.

In the present work, the complex salt bis(4,5-dihydro-1*H*-benzo[g]indazole)silver(I) nitrate, $[Ag(N_2C_{11}H_{10})_2]NO_3$, was synthesized and characterized. The optimized structure, frontier molecular orbitals (HOMO and LUMO) and global reactivity descriptors were investigated by performing DFT calculations.

2. Experimental Section

2.1. Materials and Experimental Procedures

All chemicals were purchased from Aldrich and used as received. The ligand, 4,5-dihydro-1*H*-benzo[g]indazole was prepared following Trofimenko reported procedure [16]. The synthesis of the complex was carried out in air. Melting point was uncorrected and measured using an SMP3 Stuart Scientific instrument operating at a ramp rate of 1.5˚C /min. Elemental analysis (C, H, N) was performed with a Fisson Instrument 1108 CHNS-O elemental analyzer, while the thermogravimetric analysis was obtained using a Perkin-Elmer STA 6000 thermo-balance. The IR spectrum was recorded from 4000 - 650 cm^{-1} with a Perkin-Elmer System 100 FT-IR spectrophometer. ^{1}HNMR spectrum was recorded on a Mercury Plus Variant 400 spectrophotometer operating at room temperature. Proton chemical shift (δ) values are reported in parts per million (ppm) from $SiMe_4$ (calibrating by internal deuterium solvent lock). Peak multiplicities are abbreviated as: singlet, s; doublet, d; triplet, t; quartet, q and multiplet, m. Crystal of the new compound coated with dry perfluoropolyether were mounted on a glass fiber and fixed under a cold nitrogen stream. The intensity data were collected on a Bruker-Nonius X8ApexII CCD area detector diffractometer using Mo-K_α-radiation source (λ = 0.71073 Å) fitted with a graphite monochromator. The data collection strategy used was ω and φ rotations with narrow frames (width of 0.50 degree). Instrument and crystal stability were evaluated from the measurement of equivalent reflections at different measuring times and no decay was observed. The data were reduced using SAINT [17] and corrected for Lorentz and polarization effects, and a semiempirical absorption correction was applied (SADABS) [18]. The structure was solved by direct methods using SIR-2002 [19] and refined against all F^2 data by full-matrix least-squares tech-

niques using SHELXL-2016/6 [20] minimizing $w[Fo^2\text{-}Fc^2]^2$. All the non-hydrogen atoms were refined with anisotropic displacement parameters. The hydrogen atoms of the compound were included from calculated positions and allowed to ride on the attached atoms with isotropic temperature factors (U_{iso} values) fixed at 1.2 times those U_{eq} values of the corresponding attached atoms. The DFT calculations were performed using the Gaussian 09 Revision – A.02-SMP program [21]. The vibrational frequencies, electronic structure and geometries of the isolated compound were computed within the density functional theory (DFT) at the B3LYP level, using the LanL2DZ basis set for all the atoms. Molecular orbitals (MO) were visualized using the GaussView 5.0.8 program. Global reactivity descriptors—the chemical potential (μ), chemical hardness (η), molecular electrophilicity (ω), and chemical softness which indicate the overall stability and reactivity of the system [22] were computed directly from the energies of the highest occupied molecular orbital (HOMO) and lowest unoccupied molecular orbital (LUMO).

2.2. Synthesis of $[Ag(N_2C_{11}H_{10})_2]NO_3$

The compound Bis(4,5-dihydro-1*H*-benzo[g]indazole)silver(I) Nitrate, $[Ag(N_2C_{11}H_{10})_2]NO_3$, was synthesized by the reaction of 4,5-dihydro-1*H*-benzo[g]indazole with silver(I) nitrate in methanol, at ambient temperature according to Equation (1).

$$AgNO_3 + 2C_{11}H_{10}N_2 \xrightarrow[AT]{MeOH} \left[Ag\left(N_2C_{11}H_{10}\right)_2\right]NO_3 \quad (1)$$

In a 50 mL round bottom flask containing 25 mL of methanol was introduced 0.05 g (0.29 mmol) of silver nitrate ($AgNO_3$) which dissolved upon magnetic agitation at ambient temperature (AT) giving a colorless solution. To this solution was added 0.10 g (0.58 mmol) of 4,5-dihydro-1*H*-benzo[g]indazole ($C_{11}H_{10}N_2$) in the 1:2 ratio, which also dissolved after few minutes of agitation giving a yellow limpid solution. The resulting solution was stirred overnight and then filtered. The complete evaporation of the solvent from the mother liquor at ambient temperature (AT) gave the non-hygroscopic and air-stable yellowish crystals of $[Ag(N_2C_{11}H_{10})_2]NO_3$ in an 80% yield.

3. Results and Discussion

3.1. Physical Properties and Elemental Analysis

The synthesized complex salt, $[Ag(N_2C_{11}H_{10})_2]NO_3$ is yellowish in color and melts between 210˚C - 212˚C. The experimental values from the analysis of elements present are in conformity with the theoretical values as summarized on Table 1.

3.2. IR Spectrum of $[Ag(N_2C_{11}H_{10})_2]NO_3$

The FT-IR spectrum of $[Ag(N_2C_{11}H_{10})_2]NO_3$ displays a characteristic broad (br) absorption band at 3214 cm^{-1} attributed to the stretching vibration of N–H of the pyrazole unit [23]. The shift to higher frequencies with respect to the spec-

Table 1. Percentage of analyzed elements (C, H, N) in $[Ag(N_2C_{11}H_{10})_2]NO_3$.

Percentage of C, H, N in $[Ag(N_2C_{11}H_{10})_2]NO_3$			
	% C	% H	% N
Theoretical Values	51.78	3.95	13.72
Experimental Values	51.63	3.99	13.78

trum of the free 4,5-dihydro-1*H*-benzo[g]indazole ligand (3159 - 3062 cm^{-1}) is due to the interaction between the silver metal and the ligand molecule. The variable weak (v, w) band between 2947 cm^{-1} and 2897 cm^{-1} can be assigned to the stretching vibrations of C–H of both saturated and unsaturated carbon atoms of the ligand. The variable weak (v, w) bands between 1585 cm^{-1} and 1540 cm^{-1} can be assigned to vibrations of the C=N of the pyrazole unit and the C=C stretching of the aromatic ring [24]. The broad (br) intense absorption band at 1372 - 1283 cm^{-1} is attributable to the stretching of the non coordinated nitrate ion.

3.3. ^{1}H Nuclear Magnetic Resonance Spectrum (^{1}HNMR)

The ^{1}HNMR spectrum shows five families of protons appearing from the weak field towards the strong field as follows: a singlet at $\delta = 7.9$ ppm (2H, s) is attributable to the N–H group of the pyrazole ring, a singlet at $\delta = 7.5$ ppm (2H, s) is attributed to the N=CH- of the pyrazole ring, a multiplet at 7.2 ppm (8H, m) is characteristic of aromatic protons and two triplets at $\delta = 2.9$ ppm (4H, t) and $\delta =$ 2.7 ppm (4H, t) attributable to two methylene (CH_2-CH_2) groups of the cyclohexane ring.

3.4. Thermogravimetric Analysis

Thermal stability of the complex salt $[Ag(N_2C_{11}H_{10})_2]NO_3$ was measured from room temperature to 250˚C (**Figure 1**) under dinitrogen atmosphere. The TG analysis (curve 1) shows that $[Ag(N_2C_{11}H_{10})_2]NO_3$ is thermally stable right up to 210˚C and progressively loses weight till 250˚C. This weight loss of 27.6% cannot be attributed to a particular fragment of this complex salt molecule. In fact, at this temperature range (210˚C - 250˚C), the complex melts and decomposes. The heat change (curve 2) confirms that the melting, occurring at 210˚C with formation enthalpy of $\Delta H_f = -1.55$ KJ.mol^{-1}, is an exothermic process. Beyond 220˚C appear some perturbations on the heat change behavior of the complex salt.

3.5. Crystal Structure of $[Ag(N_2C_{11}H_{10})_2]NO_3$

Single-crystal X-ray structural analysis reveals that the title compound is a complex salt of formula, $[Ag(N_2C_{11}H_{10})_2]NO_3$, having $[Ag(N_2C_{11}H_{10})_2]^+$ as complex cation and NO_3^- as counter anion. **Figure 2** shows the MERCURY and the ORTEP views of the crystal structure of the title compound. Crystal data and structure refinement details are summarized in **Table 2** and selected bond lengths and angles are in **Table 3**.

Each cationic entity, $[Ag(N_2C_{11}H_{10})_2]^+$, consists of a central silver ion coordinated to two nitrogen atoms (N2, N4) from the pyrazole unit of two ligand molecules. As a result, the silver ion has a pseudo-linear AgN_2 coordination mode, with an N2–Ag1–N1 angle of 154.2˚ and a bond distance of N2–Ag1 = 2.194 Å, Ag1–N4 = 2.127 Å. This Ag-N bond length is similar to those found in other silver-pyrazole type complexes [25]. The pair of 4,5-dihydro-1*H*-benzo[g]indazole

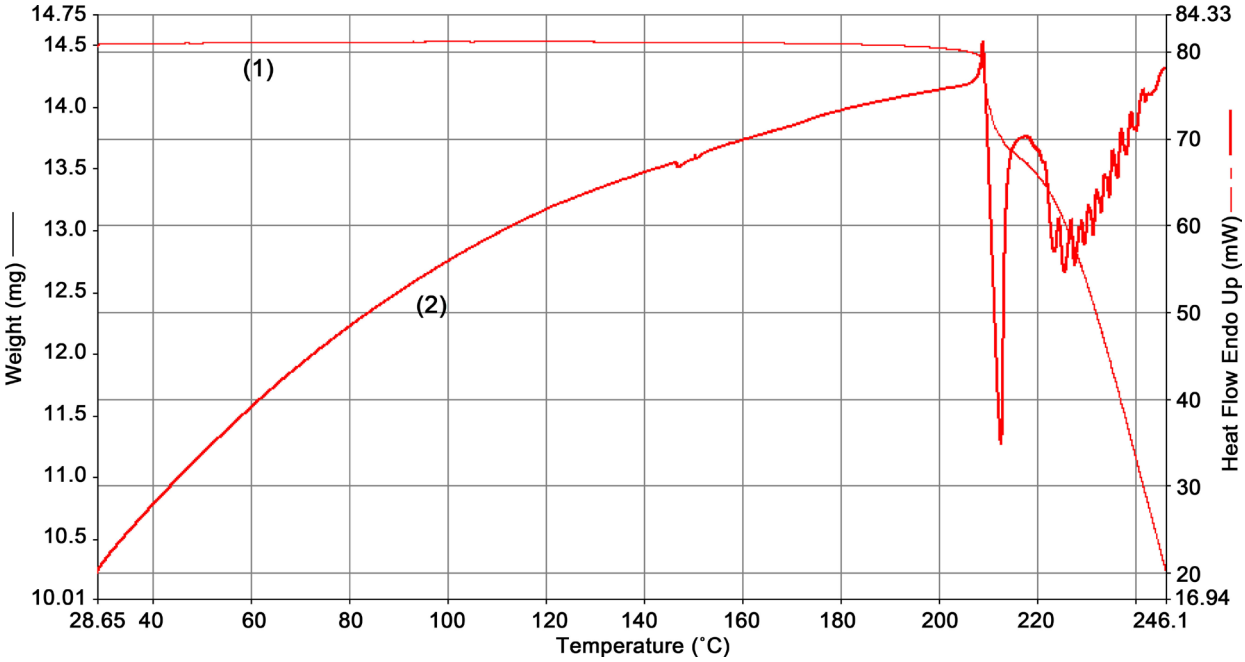

Figure 1. Thermogravimetric curve of $[Ag(N_2C_{11}H_{10})_2]NO_3$ under N_2 atmosphere.

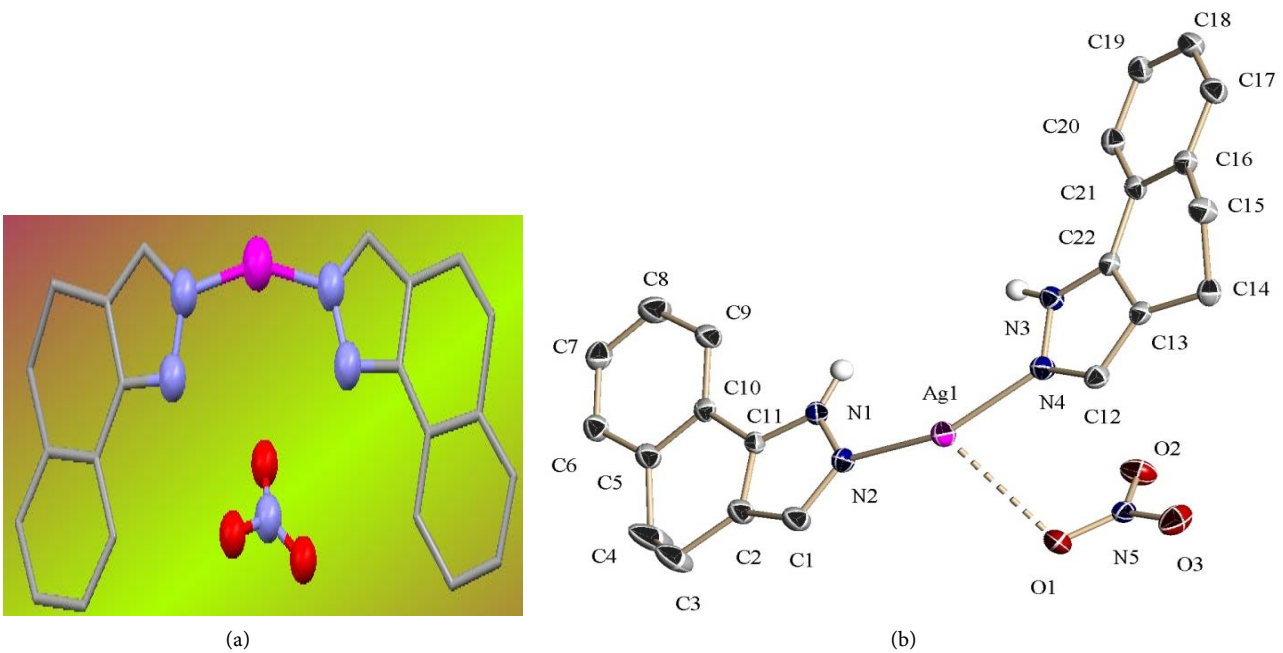

(a) (b)

Figure 2. (a) Mercury view (ball and sticks) of the molecular structure of $[Ag(N_2C_{11}H_{10})_2]NO_3$ Ag (pink), N (blue), O (red); (b) ORTEP view of the molecular structure of $[Ag(N_2C_{11}H_{10})_2]NO_3$ showing the numbering and labeling of the different atoms (hydrogen atoms have been omitted for the sake of clarity).

Table 2. Crystallographic data and structure refinement details of $[Ag(N_2C_{11}H_{10})_2]NO_3$.

Empirical formula	$C_{22}H_{20}AgN_5O_3$	
Formula weight	510.30	
Temperature	173(2) K	
Wavelength	0.71073 Å	
Crystal system	Monoclinic	
Space group	$P2_1/c$	
Unit cell dimensions	a = 7.6422(6) Å	α = 90°.
	b = 9.8237(8) Å	β = 97.041(3)°.
	c = 26.322(2) Å	γ = 90°.
Volume	1961.2(3) $Å^3$	
Z	4	
Density (calculated)	1.728 Mg/m^3	
Absorption coefficient	1.065 mm^{-1}	
F(000)	1032	
Crystal size	0.600 × 0.250 × 0.240 mm^3	
Theta range for data collection	1.559˚ to 25.249˚.	
Index ranges	$-8 \le h \le 9$, $-10 \le k \le 11$, $-31 \le l \le 21$	
Reflections collected	14,790	
Independent reflections	3457 [R(int) = 0.0329]	
Completeness to theta = 25.242˚	97.5%	
Absorption correction	Semi-empirical from equivalents	
Max. and min. transmission	0.9912 and 0.9572	
Refinement method	Full-matrix least-squares on F^2	
Data/restraints/parameters	3457 / 2 / 286	
Goodness-of-fit on F^2	1.069	
Final R indices [I > 2sigma(I)]	R_1 = 0.0392, wR_2 = 0.0976	
R indices (all data)	R_1 = 0.0491, wR_2 = 0.1030	
Extinction coefficient	n/a	
Largest diff. peak and hole	1.259 and −0.747 e.$Å^{-3}$	

Table 3. Selected bond lengths and angles in the title compound.

Bonds	Lengths (Å)	Angles	Values (˚)
Ag(1)–N(2)	2.194(3)	N(2)–Ag(1)–N(4)	154.22(11)
Ag(1)–N(4)	2.127(3)	C(11)–N(1)–N(2)	110.9(3)
		C(1)–N(2)–Ag(1)	132.4(2)
		C(1)–N(2)–Ag(1)	121.9(2)
		N(1)–N(2)–Ag(1)	117.37(3)

ligands bonded to the Ag center is arranged such that the nitrogens bearing H atoms in each ligand lie on the same side of the pseudo-linear Ag–N bonds. This geometry adopted by silver is similar to that observed by Crawford and his co-workers in the complex salt, bis(3,5-dimethyl-1*H*-pyrazole-κ*N*²)silver(I) hexaf-

luoridoantimonate ($[Ag(N_2C_5H_8)_2]SbF_6$) in which N2–Ag1–N2 angle is rather 176.54˚ [26]. Detailed analysis of the crystal packing of the salt $[Ag(N_2C_{11}H_{10})_2]NO_3$ reveals that the NO_3^- anion does not act as coordinated ligand, but rather is involved in hydrogen bonds N–H···O: 2.07Å and weak interactions: Ag···O: 3.0 Å (**Figure 3(a)** and **Figure 3(b)** and **Table 4**. In addition to these interactions, there are other non-covalent intermolecular interactions such as Ag···π: 3.4 Å and C–H···π: 2.8 Å as depicted in **Figure 4(a)** and **Figure 4(b)** involving the π–electron of cyclohexene ring and either silver metal or the hydrogen atom belonging to the neighboring pyrazole.

The NO_3^- anion is linked to the cation complex through electrostatic interactions, intermolecular N–H···O and Ag···O interactions. The bulk structure is consolidated by N–H···O, C–H···π Ag···π and Ag···O intermolecular interactions, thus generating a helical crystalline network, as shown in **Figure 5**.

3.6. DFT Studies

The DFT calculations were performed at the B3LYP level in the gas phase using

Table 4. Hydrogen bond lengths (Å) and angles (˚) for the title compound.

D–H···A	d(D–H)	d(H···A)	d(D···A)	<(DHA)>
N(3)–H(3N)···O(2)#1	0.916(18)	2.07(2)	2.973(4)	168(3)
N(1)–H(1N)···O(2)#1	0.894(18)	2.07(2)	2.897(4)	154(4)

Symmetry transformations used to generate equivalent atoms: #1 −x + 1, y-1/2, −z + 1/2.

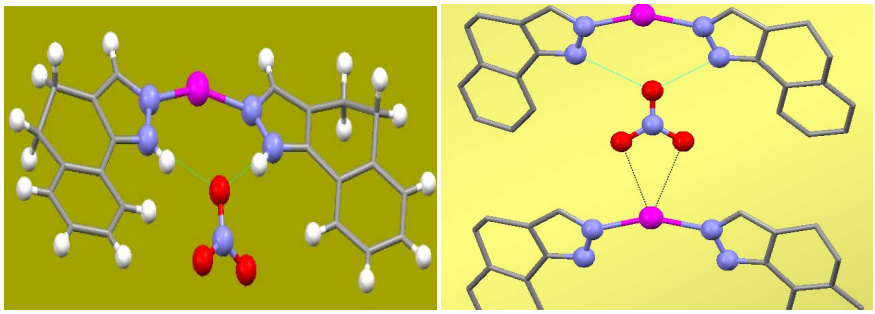

(a) (b)

Figure 3. (a) N–H···O (2.07Å) intermolecular hydrogen bonds; (b) weak Ag···O (3.0 Å) interactions.

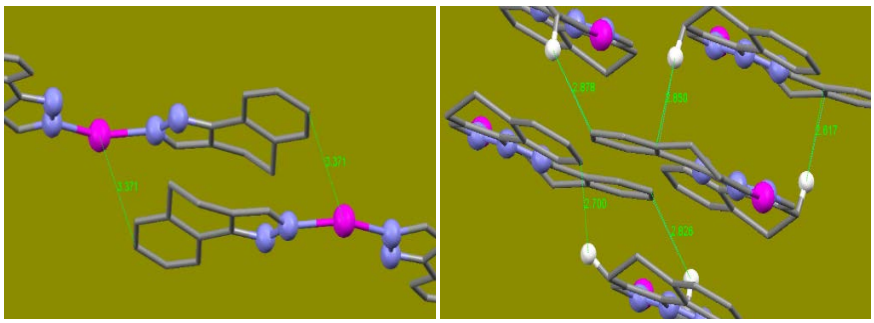

(a) (b)

Figure 4. (a) Ag···π (3.4 Å) and (b) C–H···π (2.8 Å) intermolecular interactions.

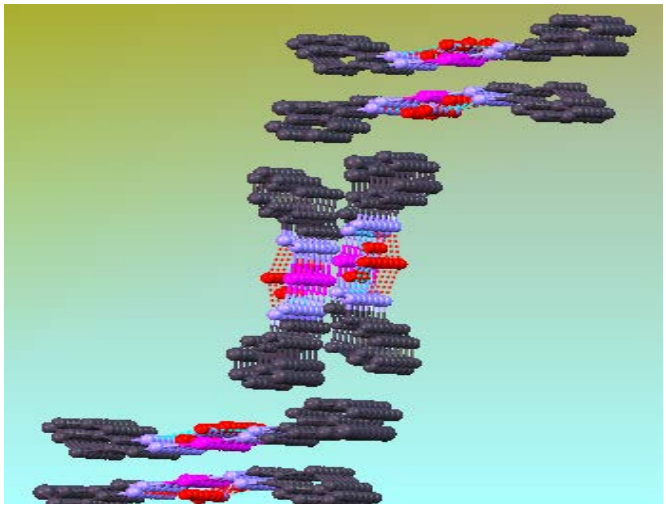

Figure 5. Pseudo-helical crystalline network in $[Ag(N_2C_{11}H_{10})_2]NO_3$.

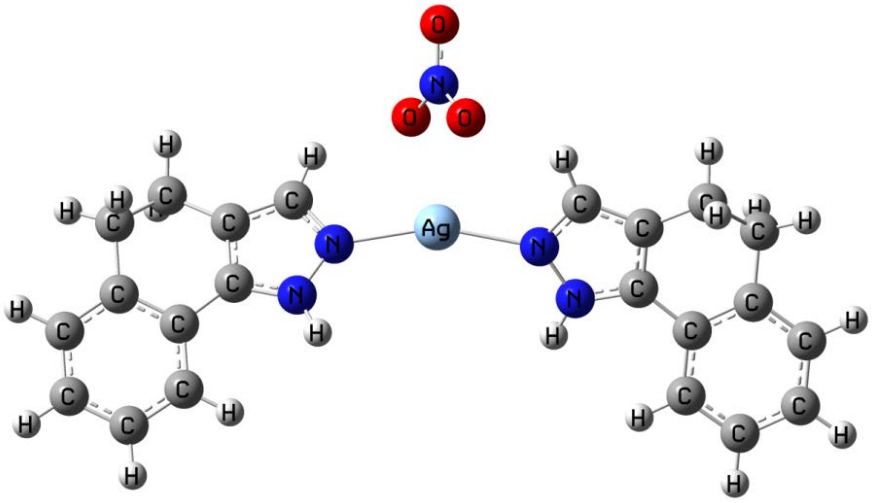

Figure 6. Optimized structure of $[Ag(N_2C_{11}H_{10})_2]NO_3$.

the LanL2DZ basis set, in order to understand the structural preferences of the atoms in the $[Ag(N_2C_{11}H_{10})_2]NO_3$ complex salt. The resulting optimized structure is shown in Figure 6.

The π-electron system in the pyrazole unit and the benzene fraction of the ligands observed in the experimental structure are well localized in the optimized structure. The reproducibility of the experimental geometry is quite satisfactory. A comparison of the experimental and theoretical geometric parameters of the compound is illustrated on Table 5.

It is observed that some slight changes occurred in the geometry of $[Ag(N_2C_{11}H_{10})_2]NO_3$ after optimization. The Ag1–N2 and Ag1–N4 bond lengths increase from 2.127 Å to 2.211 Å and from 2.194 Å to 2.211 Å respectively. The computed C11–N1, C3–C4, C10–C11, N5–O2 and N5–O3 bonds appear overestimated with a discrepancy ranging from 0.102 to 0.149 Å while the remaining bond lengths agree within 0.073 Å. Selected dihedral angles between various atomic planes are presented in Table 6 and FT-IR vibrational frequencies of

Table 5. Comparison between experimental and theoretical geometric parameters of $[Ag(N_2C_{11}H_{10})_2]NO_3$.

Bond	Experimetal Length (Å)	Theoretical Length (Å)	Difference between Experimental and Theoretical Lengths (Å)
Ag1–N2	2.127	2.211	0.084
Ag1–N4	2.194	2.211	0.017
N1–N2	1.369	1.387	0.018
C11–N1	1.478	1.376	0.102
N2–C1	1.354	1.360	0.006
C1–C2	1.402	1.416	0.014
C2–C11	1.382	1.402	0.020
N4–C12	1.349	1.360	0.011
C12–C13	1.360	1.416	0.056
C13–C22	1.366	1.402	0.036
C22–N3	1.429	1.376	0.053
N3–N4	1.367	1.387	0.020
N5–O1	1.328	1.328	0.00
N5–O2	1.129	1.278	0.149
N5–O3	1.208	1.328	0.120

Table 6. Dihedral angles between some atomic planes in $[Ag(N_2C_{11}H_{10})_2]NO_3$.

Atoms	Dihedral Angles (˚)	Atoms	Dihedral Angles (˚)
Ag1–N2–N1–C11	176.46	C11–C2–C3–C4	30.32
Ag1–N2–C1–C2	−176.85	N1–N2–Ag1–N4	25.24
Ag1–N4–N3–C22	176.46	N2–Ag1–N4–N3	24.97
Ag1–N4–C12–C13	176.84	C1–N2–Ag1–N4	−158.19
N2–N1–C11–C2	0.40	N2–Ag1–N4–N3	−158.47
N2–C1–C2–C11	−0.25	N4–C12–C13–C22	−0.25
N1–C11–C2–C1	−0.09	N4–N3–C22–C13	0.40
N1–C11–C2–C3	178.40	N3–N4–C12–C13	0.48
N2–C1–C2–C3	−178.45	N3–C22–C13–C12	−0.09

$[Ag(N_2C_{11}H_{10})_2]NO_3$ in **Table 7**.

The DFT studies show that $Ag(N_2C_{11}H_{10})_2]NO_3$ has 332 molecular orbitals (MOs), with 115 occupied MOs and 217 unoccupied MOs. The highest occupied molecular orbital, HOMO is the 115th MO (**Figure 7(a)**) and has an energy of −129.85 Kcal/mol while the lowest unoccupied molecular orbital, LUMO which is the 116th MO (**Figure 7(b)**), has an energy of -37.71 Kcal/mol. The red regions represent the positive phases of the molecular orbitals while the green ones represent the negative phases. Significant contributions to the highest occupied molecular orbitals (HOMOs) come from the orbitals of the metal and the nitrate

ion, with some small contributions coming from the nitrogen atoms of the ligands which are bonded to the metal center. Also, the orbitals of the ligand molecules make the main contributions to the lowest unoccupied molecular orbitals (LUMOs) with small contributions from the orbitals of the central metal.

Table 7. Calculated IR vibrational frequencies (cm^{-1}) of $[Ag(N_2C_{11}H_{10})_2]NO_3$ complex salt and their assignment.

Calculated Frequencies (cm^{-1})	Vibrational Assignment
3707.1	$(N–H)_{pyrazole}$ stretching vibration
3279.2	$(C–H)_{pyrazole}$ stretching vibration
3230.3	$(C–H)_{benzene}$ stretching vibration
3114.4	$(C–H)_{cyclohexane}$ anti-symmetric stretching
1661.5	$(C–C,C=C)_{cyclohexane,\ benzene}$ anti-symmetric stretching
1501.0	$(C–H)_{cyclohexane,\ benzene}$ scissoring
1435.3	$(C=C)_{pyrazole}$ stretching
1377.6	$(NO_3^-)_{uncoordinated}$ anti-symmetric stretching
1324.1	$(C–H)_{cyclohexane,\ benzene}$ rocking
1095.7	$(C=N, N–N)_{pyrazole}$ symmetric stretching
1062.3	$(C–C)_{cyclohexane}$ twisting
1033.1	$(C=C)_{benzene}$ twisting
979.3	$Ag–N_{pyrazole}$ symmetric stretching
968.4	$(C–H)_{pyrazole}$ rocking
959.8	$(NO_3^-)_{uncoordinated}$ symmetric stretching
802.9	$(C–H)_{benzene}$ wagging
720.5	$(NO_3^-)_{uncoordinated}$ wagging
647.7	$(NO_3^-)_{uncoordinated}$ scissoring
574.1	$(N–H)_{pyrazole}$ rocking
434.1	$(C–C)_{cyclohexane}$ scissoring
183.4	$Ag–N_{pyrazole}$ anti-symmetric stretching

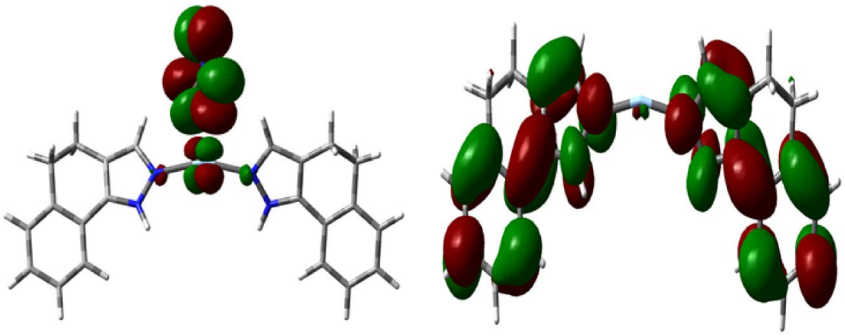

(a) (b)

Figure 7. Pictural view of (a) highest occupied molecular orbitals and (b) lowest unoccupied molecular orbitals of $[Ag(N_2C_{11}H_{10})_2]NO_3$.

Table 8. Global reactivity descriptors for the title complex.

Gobal reactivity descriptor	Value
Ionization energy (I) (Kcal/mol)	129.85
Electron affinity (A) (Kcal/mol)	37.71
Chemical potential (μ) (Kcal/mol)	83.78
Chemical hardness (η) (Kcal/mol)	46.07
Chemical softness (*S*) (mol/Kcal)	0.01
Electrophilicity index (ω) (Kcal/mol)	76.18

Some global reactivity descriptors of the complex salt obtained from theoretical calculations are summarized on Table 8.

4. Conclusions

The new complex salt, bis(4,5-dihydro-1*H*-benzo[g]indazole)silver(I) nitrate, $[Ag(N_2C_{11}H_{10})_2]NO_3$, has been synthesized and characterized. This compound presents an interesting two-dimensional pseudo-helical network based on the self-assembly of ionic units through coulombic and N–H···O, C–H···π, Ag···π and Ag···O intermolecular interactions. Thermal analysis reveals that the compound is stable up to *ca.* 210˚C. DFT results show some discrepancies between the X-ray and the optimized structures in terms of bond lengths and angles. The Ag^+ cation and the NO_3^- ion make the major contributions to HOMO, while the $C_{11}H_{10}N_2$ ligands make significant contributions to LUMO. However, the reactivity of this complex salt cannot be directly induced, but can be compared with the reactivity of other related complexes.

Preliminary observations from our laboratory promisingly suggest that a well-conceived and systematically conducted preparative procedure may be applied generally to fabricate a whole range of homologous materials.

Acknowledgements

The authors are grateful to Prof E. Alvarez of Instituto de Investigaciones Quimicas (IIQ)-Universidad de Sevilla (Spain) for X-ray facilities and to Prof C. Pettinari of the University of Camerino (Italy) for spectroscopic and Thermogravimetric analyses facilities.

References

[1] Sultivan, T.J., Truglio, J.J., Boyne, M.E., Novichenok, P., Zhang, X., Stratton, C.F., Li, H.J., Kaur, T., Amin, A., Johnson, F., Stayden, R.A., Kisker, C. and Tonge, P.J. (2006) High Affinity InhA inhibitors with Activity Against Drug-Resistant Strains of *Mycobacterium tuberculosis*. *ACS Chemical Biology*, **1**, 43-53. https://doi.org/10.1021/cb0500042

[2] Prakash, O., Pundeer, R., Ranjan, P., Pannu, K., Dhingra, Y. and Aneja, K.R. (2009) Synthesis and Antibacterial Activity of 1,3-Diaryl-4-Cyanopyrazoles. *Indian Journal of Chemistry*, **48B**, 563-568.

[3] Magedov, I.V., Manpadi, M., Slambrouck, S.V., Steelant, W.F., Rozhkova, E.,

Przheval'skii, N.M., Rogelj, S. and Kornienko, A. (2007) Discovery and Investigation of Antiproliferative and Apoptosis-Inducing Properties of New Heterocyclic Podophyllotoxin Analogues Accessible by a One-Step Multicomponent Synthesis. *Journal of Medicinal Chemistry*, **50**, 5183-5192. https://doi.org/10.1021/jm070528f

[4] Soliman, R., Habib, N.S., Ashour, F.A. and El-Taiebi, M. (2001) Synthesis and Antimicrobial Activity of Novel Pyrazole, Pyrazoline, Pyrazolinone and Pyrazolidinedione Derivatives of Benzimidazole. *Bollettino Chimico Farmaceutico*, **140**, 140-148.

[5] Liu, X.H., Cui, P., Song, B.A., Bhadury, P.S. Zhu, H.L. and Wang, S.F. (2008) Synthesis, Structure and Antibacterial Activity of Novel 1-(5-Substituted-3-substituted-4,5-dihydropyrazol-1-yl)Ethanone Oxime Ester Derivatives. *Bioorganic & Medicinal Chemistry*, **16**, 4075-4082.

[6] Sener, A., Sener, M.K., Bildmci, I., Kasimogullari, R. and Akcamur, Y. (2002) Studies on the Reactions of Cyclic Oxalyl Compounds with Hydrazines or Hydrazones II: Synthesis and Reactions of 4-Benzoyl-1-(3-nitrophenyl)-5-phenyl-1*H*-pyrazole-3-carboxylic Acid. *Journal of Heterocyclic Chemistry*, **39**, 869-875. https://doi.org/10.1002/jhet.5570390503

[7] Menozzi, G., Mosti, L., Schenone, P., D'Amico, M., Falciani, M. and Filippelli, W. (1994) 1-Aryl-1H-pyrazole-5-acetic Acids with Anti-Inflammatory, Analgesic and Other Activities. *Farmaco*, **49**, 115-119.

[8] Barszcz, B. (2005) Coordination Properties of Bidentate N,O Heterocyclic Alcohols and Aldehydes Towards Cu(II), Co(II), Zn(II) and Cd(II) Ions in the Solid State and Aqueous Solution. *Coordination Chemistry Reviews*, **249**, 2259-2276.

[9] Zora, M., Pinar, A.N., Odabaşoğlu, M., Büyükgüngör, O. and Turgut, G. (2008) Synthesis of Ferrocenyl Pyrazoles by the Reaction of 3-Ferrocenylpropynal with Hydrazinium Salts. *Journal of Organometallic Chemistry*, **693**, 145-314.

[10] Ngoune, J. (2008) New Hybrid Metal-Organic Materials Polyfunctional Containing, N-Donor Ligand. Ph.D. Thesis, University of Camerino, Camerino, Italy.

[11] Qian, J., Liu, Y., Zhu, J., Jiang, B. and Xu, Z. (2011) A Novel Synthesis of Fluorinated Pyrazoles via Gold(I)-Catalyzed Tandem Aminofluorination of Alkynes in the Presence of Selectfluor. *Organic Letters*, **13**, 4220-4223. https://doi.org/10.1021/ol201555z

[12] Trofimenko, S. (1972) The Coordination Chemistry of Pyrazole-Derived Ligands. *Chemical Reviews*, **72**, 497-509. https://doi.org/10.1021/cr60279a003

[13] Ten-Hoedt, R.W., Driessen, W.L. and Verschoor, G. (1983) Structure of Hexakis(pyrazole)nickel(II) Bis(tetrafluoroborate), $[Ni(C_3H_4N_2)_6](BF_4)_2$. *Acta Crystallographica*, **C39**, 71-72.

[14] Casarin, M., Forrer, D., Garau, F., Pandolfo, L., Pettinari, C. and Vittadini, A. (2009) Tris(pyrazol-1-yl)borate and Tris(pyrazol-1-yl)methane: A DFT Study of Their Different Binding Capability toward Ag(I) and Cu(I) Cations. *Inorganica Chimica Acta*, **362**, 4358-4364.

[15] Santos, C., Gómez, M., Álvarez, E., Ngoune, J., Marchetti, F., Pettinari, R. and Pettinari, C. (2016) Group 9 and 10 Complexes with the Bidentate Di(1*H*-indazol-1-yl)methane and Di(2*H*-indazol-2-yl)methane Ligands: Synthesis and Structural Characterization. *New Journal of Chemistry*, **40**, 5695-5703. https://doi.org/10.1039/C5NJ03135D

[16] Rheingold, A.L., Ostrander, R.L., Haggerty, B.S. and Trofimenko, S. (1994) Homoscorpionate (Tris(pyrazolyl)borate) Ligands Containing Tethered 3-Phenyl Groups. *Inorganic Chemistry*, **33**, 3666-3676. https://doi.org/10.1021/ic00095a009

[17] (2007) APEX2. Bruker AXS Inc., Madison, Wisconsin, USA.

[18] (2004) Bruker Advanced X-Ray Solutions. SAINT and SADABS Programs. Bruker AXS Inc., Madison, Wisconsin, USA.

[19] Burla, M.C., Camalli, M., Carrozzini, B., Cascarano, G.L., Giacovazzo, C., Polidori, G. and Spagna, R. (2003) SIR2002: The Program. *Journal* of *Applied Crystallography*, **36**, 1103. https://doi.org/10.1107/S0021889803012585

[20] Sheldrick, G.M. (2015) Crystal Structure Refinement with *SHELXL. Acta Crystallographica*, **C71**, 3-8.

[21] Amsterdam Density Functional (ADF) Version 2007.01. http://www.scm.com

[22] Umadevi, P. and Lalitha, P. (2012) Synthesis and Antimicrobial Evaluation of Imino Substituted 1, 3, 4 Oxa and Thiadiazoles. *International Journal of Pharmacy and Pharmaceutical Sciences.* **4**, 523-527.

[23] Gunasekaran, S. and Anita, B. (2008) Spectral Investigation and Normal Coordinate Analysis of Piperazine. *Indian Journal of Pure & Applied Physics*, **46**, 833-838.

[24] Nakamoto K. (1997) Infrared Spectra of Inorganic and Coordination Compounds. Wiley, New York.

[25] Baran, E.J. (2005) The Saccharinate Anion: A Versatile and Fascinating Ligand in Coordination Chemistry. *Química Nova*, **28**, 326-328. https://doi.org/10.1590/S0100-40422005000200025

[26] Crawford, D., Hofer, A.K., Edler, K.L. and Ferrence, G.M. (2011) Bis(3,5-dimethyl-1H-pyrazole-κN^2)silver(I) Hexafluoridoantimonate. *Acta Crystallographica*, **E67**, m496. https://doi.org/10.1107/s1600536811010567

Supplementary Material

Detailed crystallographic data in CIF format for this paper were deposited with the Cambridge Crystallographic Data Centre (CCDC-1547647). The data can be obtained free of charge at http://www.ccdc.cam.ac.uk/conts/retrieving.html [or from Cambridge Crystallographic Data Centre (CCDC), 12 Union Road, Cambridge CB2 IEZ, UK; fax: +44 (0) 1223-336033; e-mail: deposit@ccdc.cam.ac.uk].